



**HAL**  
open science

## Direct growth of carbon nanotubes forests on carbon fibers to replace microporous layers in proton exchange membrane fuel cells

Marie Fontana, Raphaël Ramos, Arnaud Morin, Jean Dijon

### ► To cite this version:

Marie Fontana, Raphaël Ramos, Arnaud Morin, Jean Dijon. Direct growth of carbon nanotubes forests on carbon fibers to replace microporous layers in proton exchange membrane fuel cells. *Carbon*, 2021, 172, pp.762 - 771. 10.1016/j.carbon.2020.10.049 . hal-03493137

**HAL Id: hal-03493137**

**<https://hal.science/hal-03493137>**

Submitted on 7 Nov 2022

**HAL** is a multi-disciplinary open access archive for the deposit and dissemination of scientific research documents, whether they are published or not. The documents may come from teaching and research institutions in France or abroad, or from public or private research centers.

L'archive ouverte pluridisciplinaire **HAL**, est destinée au dépôt et à la diffusion de documents scientifiques de niveau recherche, publiés ou non, émanant des établissements d'enseignement et de recherche français ou étrangers, des laboratoires publics ou privés.



Distributed under a Creative Commons Attribution - NonCommercial 4.0 International License

**Direct growth of carbon nanotubes forests on carbon fibers to replace microporous layers in proton exchange membrane fuel cells.**

Marie Fontana<sup>a</sup>, Raphaël Ramos<sup>a</sup>, Arnaud Morin<sup>a\*</sup>, Jean Dijon<sup>a</sup>

<sup>a</sup> Univ. Grenoble Alpes, CEA, LITEN, F-38000 Grenoble, France

\*Arnaud Morin : +33 438785986, [arnaud.morin@cea.fr](mailto:arnaud.morin@cea.fr)

## Abstract

A novel microporous layer structure for fuel cell application has been developed based on the direct growth of thin multiwall carbon nanotubes forests on the carbon fiber support of a commercial gas diffusion media free of hydrophobic treatment. The growth process is a hot filaments assisted chemical vapor deposition coupled with a specific catalyst dedicated to the growth of carbon nanotubes on carbon support. The so obtained carbon nanotube forests are perpendicularly aligned all along the carbon fibers and cover the surface of the gas diffusion media, providing a unique new structure of microporous layer. The carbon nanotubes composing the forests are about 10  $\mu\text{m}$  to 20  $\mu\text{m}$  long, with about 6 walls for an average diameter of 7.5 to 8 nm. Fuel cell testing demonstrated a performance improvement up to 30% compared to the best state of the art gas diffusion media, even in the presence of liquid water in the fuel cell, which is the main issue limiting performances.

## 1-Introduction

Proton Exchange Membrane Fuel Cells (PEMFC) convert electrochemical energy into electricity. This system uses  $H_2$  and air as reactants and produces water, heat and power (*figure 1*). Nevertheless, fuel cells still need to be improved in order to be economically relevant. To that purpose, it is needed to produce more power while reducing the use of materials and the size of the fuel cells. Producing more power means increasing the flows through the fuel cell, particularly gases and water flows. This implies that reactants must reach the catalytic sites even in the presence of an important amount of water inside the fuel cell core. Not only, water is produced at the cathode side where the oxygen reduction reaction (ORR) occurs, but it is also needed to hydrate the membrane and ensure proton migration. Water distribution in PEM fuel cells has been widely observed, and most of the water tends to accumulate in the cathode side [1]–[6]. When water accumulates in this area, the catalytic sites are flooded [7], [8] which prevents the reactants to reach them. Water management is then a challenge for further fuel cell development. The first step to understand water management issue is to look into the fuel cell components that water crosses.

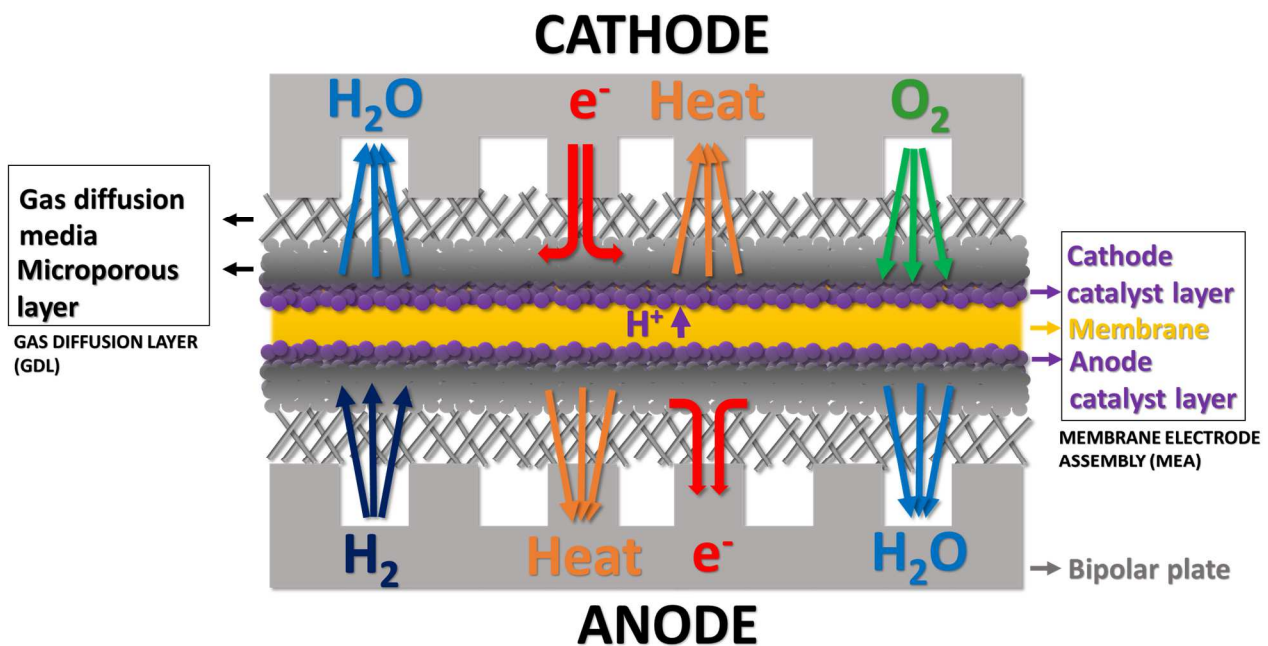


**Figure 1: Cross section of a PEM fuel cell showing the path of flows through its inner structure.**

*Figure 1* describes the fuel cell components and the flows that cross them. The central part is called the membrane-electrode assembly, or MEA, with the proton conducting membrane and the catalyst layers (anode and cathode). The most efficient and commonly used catalysts for

PEMFC are platinum-based catalysts due to their high catalytic activity for oxygen reduction (cathode) and hydrogen oxidation (anode) [9]. On both sides of the MEA are the gas diffusion layers, or GDL. These are one of the critical component in the fuel cell as all the flows (heat, gases, water, and electrons) have to pass through this layer. the most commonly used GDL is composed of a highly porous carbon fiber support, which is called gas diffusion media or GDM (150 $\mu$ m to 200 $\mu$ m thick) coated on one side by a so-called microporous layer (MPL) (up to 50 $\mu$ m thick). Alternate carbon structures are also studied [10, 11]. In the following sections, the term GDM will be used to name the carbon support and the term GDL will be used to name the assembly of a GDM and a MPL. The MPL is mainly composed of carbon black and a hydrophobic agent such as polytetrafluoroethylene (PTFE). Most studies about the microporous layer concentrate on the PTFE loading and the density of carbon black [10]–[12], but no other structures have been suggested so far. It is commonly acknowledged that the microporous layer is necessary, especially when liquid water is present in the fuel cell. The fundamental mechanisms explaining its role differ from one study to another. For example, in [8] and [7] the presence of the MPL avoided the formation of a liquid water barrier between the catalyst layer and the gas diffusion media, thus preventing the flooding of the catalytic sites and providing a better access of O<sub>2</sub> to them. More recently, limitation of the role of the MPL was evidenced in [6], where the MPL does not fully prevent the cathode side from water saturation at high relative humidity (100% RH). Improved materials for PEMFCs, managing both high gas diffusion and adequate water transport, are highly needed for performance improvement. Thus, it appears to be relevant to develop new microstructures of MPL, with the aim to improve fuel cell performances. A very different MPL microstructure could also provide another tool to understand the relationship between the media microstructure and electrochemical performances. This is the goal of the present study focused on the development of a new MPL structure based on vertically aligned carbon nanotubes grown on GDM.

Carbon nanotubes (CNTs) have already been used in the fuel cell field and a few studies in particular showed the suitability of carbon nanotubes as a material for the MPL. The use of carbon nanotubes in the microporous layer can be sorted in two categories: carbon nanotubes used in the bulk form or carbon nanotubes directly grown on the gas diffusion media. Bulk carbon nanotubes present the advantage to be commercially available in high quantities. They are generally mixed with a usual MPL formulation of carbon black and PTFE. In [13], it is observed that the use of dispersed carbon nanotubes in a carbon black mixture leads to a performance enhancement of the fuel cell. This was attributed to a better

electronic conductivity and enhanced water and gas transport through the porous layers. Carbon nanotubes increased the mean pore size diameter and enhanced liquid permeability, which leads to higher fuel cell performances than their reference material. In [14], the use of an adequate mixing ratio of CNTs and acetylene black in the MPL composition leads to a fuel cell performance improvement and a higher electrochemically active catalyst area compared to their reference material. In [15] a fuel cell performance improvement of 12% to 29% was obtained using CNTs in the MPL composition. This was attributed to the formation of through plane 3D-structures (to form gas or water preferential pathways) in the MPL which leads to a lower mass transport resistance in their case. In [16] performance improvement under both dry and wet conditions were achieved by using various loading of CNTs in the MPL. Performance improvement in dry conditions is attributed to the decrease in hydrophobicity of the MPL with CNTs, which keeps the membrane hydrated. In wet conditions, the authors achieved higher performances with a loading of CNTs in the MPL different than in dry conditions. The difference in the adequate CNT loading for performance improvement in dry or wet conditions is attributed to the change of the mean flow pore diameter in the MPL, depending on the CNT loading. More recently in [17], a microporous layer composed of a mixture of carbon black, PTFE and CNTs was deposited on the commercial support Sigracet 25BN. The authors observed that using CNTs provided a higher porosity and larger pores than a conventional MPL. Their MPL with CNTs also leads to higher performances than a conventional MPL on the same support.

Contrary to the use of bulk carbon nanotubes in MPL, only few studies describe the direct growth of carbon nanotubes to replace the microporous layer. In [18] a Co-Ni catalyst is used for CNT growth on the carbon fibers of a carbon paper. The authors obtained large multiwall carbon nanotubes with diameters in the 30 to 40 nm range. These short and curly carbon nanotubes covers the surface of the carbon fibers composing the gas diffusion media. Wet proofing treatment was applied on the CNTs. Electrochemical measurements show a performance improvement compared to carbon paper without nanotubes nor MPL. In [19], curly-shaped CNTs with a diameter of 40 nm are obtained as in [18], but no wet proofing was applied. Electrochemical measurements were conducted and compared to a carbon paper coated with carbon slurry and PTFE as a reference. Better performances were obtained for  $RH < 70\%$ . For  $RH > 70\%$ , lower performances than the reference material were obtained, and this was attributed to the absence of hydrophobic treatment leading to a higher sensitivity to flooding.

The lack of studies about the direct growth of carbon nanotubes on GDMs is related to the difficulty to grow CNTs on carbon substrates [20]. The major problem stands in the diffusion of the catalyst particles inside and on the surface of the substrate which limits the catalytic growth of CNT [21], [22]. Several studies describe the various trials of carbon nanotubes growth on carbon supports but few of them obtained vertically aligned carbon nanotubes structures on the fibers. In [22], the carbon nanotubes growth by thermal CVD on graphite fibers is achieved. Using a wide range of growth conditions, the authors showed that the catalyst particles tend to diffuse in the substrate at high growth temperatures, thus preventing carbon nanotubes growth. Nevertheless, they obtained carbon nanotubes for a range of temperatures between 650°C to 800°C. These CNTs are forming a fuzzy foam around the fibers. In [23] the carbon nanotubes growth on carbon fibers is achieved with the floating catalyst method and the length of carbon nanotubes was related to the growth temperature. The authors managed to obtain quite aligned carbon nanotubes bundles but only on small specific areas on the fibers. Several other studies describe similar results [24]–[26] of fuzzy carbon nanotubes dispersed around the carbon fibers. More recently, in [27] radially aligned carbon nanotubes were grown around pyrolytic carbon coated carbon fibers by CVD process, which might be the most aligned structure of carbon nanotubes on carbon fibers presented in the literature until now.

To the best of our knowledge, no study reports the direct growth of vertically aligned carbon nanotubes forests as obtained in our study. This paper presents a new structure of microporous layer based on an original direct growth of vertically aligned carbon nanotubes on carbon fibers, whose performances can compete with the best commercial gas diffusion layer. This paper describes first the method of the direct growth of high density vertically aligned carbon nanotubes on commercial gas diffusion media. The CNT forests are used as a MPL on the GDM and are then integrated in a single cell for fuel cell test. The electrochemical performances and durability (with a preliminary aging test) of this new structure are evaluated. It is difficult to rigorously compare studies concerning fuel cell material due to the wide variety of fuel cell test assemblies and test conditions. Also, each study compares its results to its own references. Here, a specific single differential cell and test conditions that enhance the role of the MPL allows to compare our results to the best commercially available state of the art material.

## 2 - Experimental details

The first subsection describes the method and apparatus for the growth of vertically aligned carbon nanotube forests on commercial GDM by hot filaments assisted chemical vapor deposition. The second subsection gives the experimental details for electrochemical performances evaluation of the novel MPL. The apparatus for electrochemical tests, the test conditions and the integration of the new GDM with CNTs in a single fuel cell are described.

### 2-1 Carbon nanotubes growth on carbon fibers

The catalyst layer for CNT growth is deposited by electron beam physical vapor deposition in a customized Balzers Bak-1052 device. A three-layer catalyst made of titanium (5 nm at 0.3 nm/s), aluminium (2 nm at 0.6 nm/s) and iron (1 nm at 0.3 nm/s) is deposited on the annealed gas diffusion media. These layers are deposited successively without breaking the ultrahigh vacuum. Deposition is highly directive in this equipment and the coating is only covering the accessible surface of the carbon fibers. This means that the carbon nanotubes will have the possibility to grow only on the surface of the carbon fibers exposed to the beam, and not on the full circumference of the carbon fibers.

Carbon nanotubes are grown by hot filaments assisted chemical vapor deposition (HFCVD) in a custom Plassys CVD 500 reactor. HF-CVD process consists in enhancing a classical CVD process by using hot filaments to activate the gas phase [28]–[30]. HF-CVD commonly works with metallic filaments (tungsten as an example) and is widely used for diamond growth or thin films growth [31]–[34]. Here we are however using carbon filaments instead of metallic filaments to avoid metallic contamination. The use of carbon filaments for carbon nanotubes growth has already been developed in [35]–[38] for similar reasons. Sixteen parallel carbon filaments from Poco Graphite are spring-loaded in a TiN-coated metallic holder and placed 1 cm above the sample (Fig. 2a). Filaments have a diameter of 0.5 mm and are 15 cm long. Filaments temperature is set by the electric power sent through the metallic holder, controlled by a constant current setpoint of 63 A. The reactive phase is composed of a gaseous mixture of  $C_2H_2$ ,  $H_2$  and He with a  $H_2/C_2H_2$  ratio of 157/10 and 0.9 Torr pressure.

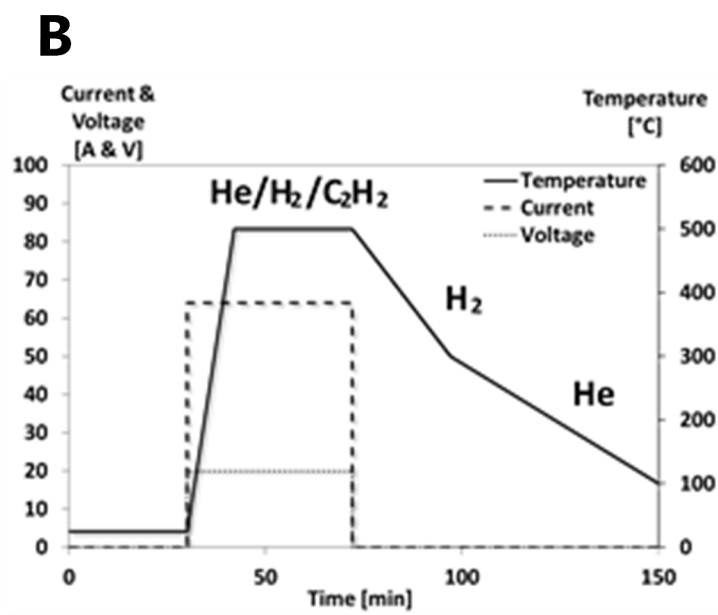
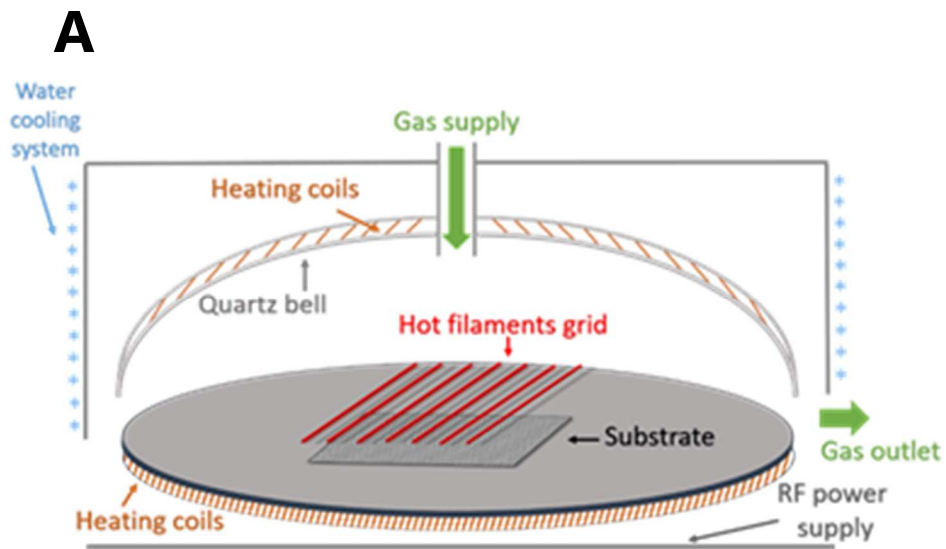


Figure 2: A) Scheme of the Hot Filaments Chemical Vapor Deposition (HF-CVD) reactor and B) HF-CVD process graph with standard conditions.

The filaments are switched on at the beginning of the heating ramp (*Figure 2B*) which is performed under reactive gas phase. The reactor temperature (substrate holder and quartz bell, *Figure 2A*) is maintained at 500°C for 30 minutes. Controlled cooling down to 300°C is then performed under H<sub>2</sub> atmosphere with the filaments switched off (*Figure 2B*). Samples are positioned under the center of the filaments grid of the reactor in order to ensure the reproducibility and the uniformity of the carbon nanotubes growths.

Gas diffusion media surface is visualized by SEM imaging on a Zeiss LEO 1530 FEG-SEM. SEM imaging delivers information on thickness, carbon fibers layout, and the carbon paper morphology. In order to obtain structural information of the nanotubes themselves, TEM analysis is conducted with a Tecnai Osiris S/TEM. The samples are observed under a 200kV acceleration voltage. TEM analysis provides information about the carbon nanotubes inner and outer diameter, and the number of walls. An adequate number of TEM images (i.e. 30 to 60) are recorded to collect data that are representative of the sample population. Diameters measurement and walls count are performed with Image J Software.

## 2-2 Electrochemical measurements

The cell hardware consisted in a gold coated aluminum plate for the anode and cathode with a machined flow field consisting in a succession of 30 parallel channels, 1.2 cm in length, 250µm in width and 400 µm in depth, with a period of 500µm corresponding to an active area of 1.8 cm<sup>2</sup> (1.2x1.5 cm<sup>2</sup>). The single cell was designed (see supplementary S1) to be a differential cell in order to provide as homogeneous operating conditions as possible on the whole active area. This means that the amounts of reactants that are consumed, and of water that is produced, in the cell during operation is negligible compared to the inlet flows. In other word, the fuel cell works at high stoichiometry, which means that the ratio between reactant supply and consumption is very high, to reduce heterogeneities from gas inlet to outlet. In addition, the pressure drop between gas inlet and outlet is negligible compared to the total pressure (few tens of mbar at the maximum). Several channels in parallel supply the reactants. The geometry of the flow field has been chosen to minimize pressure drop despite the high stoichiometric ratios. The rib/channel width is minimized to reduced rib/channel heterogeneities as observed in [6]. The reactants are flowing in opposite directions between the anode and the cathode, so called counter-flow configuration. The H<sub>2</sub> and air flows are kept constant at 35 and 95 Nl/h (normal liter per hour) respectively, corresponding to a stoichiometry of 50 at 1A/cm<sup>2</sup>. Consequently, the operating conditions, e.g. partial pressure of

products and reactants, are homogeneous from inlet to outlet. In complete fuel cells, temperature and current distribution vary locally depending on the area of the cell that is considered (close to the gas channel/rib or close to the gas supply/evacuation) [39]–[43]. It was thus important to design a differential cell to provide homogeneous functioning in order to facilitate results interpretation and understanding.

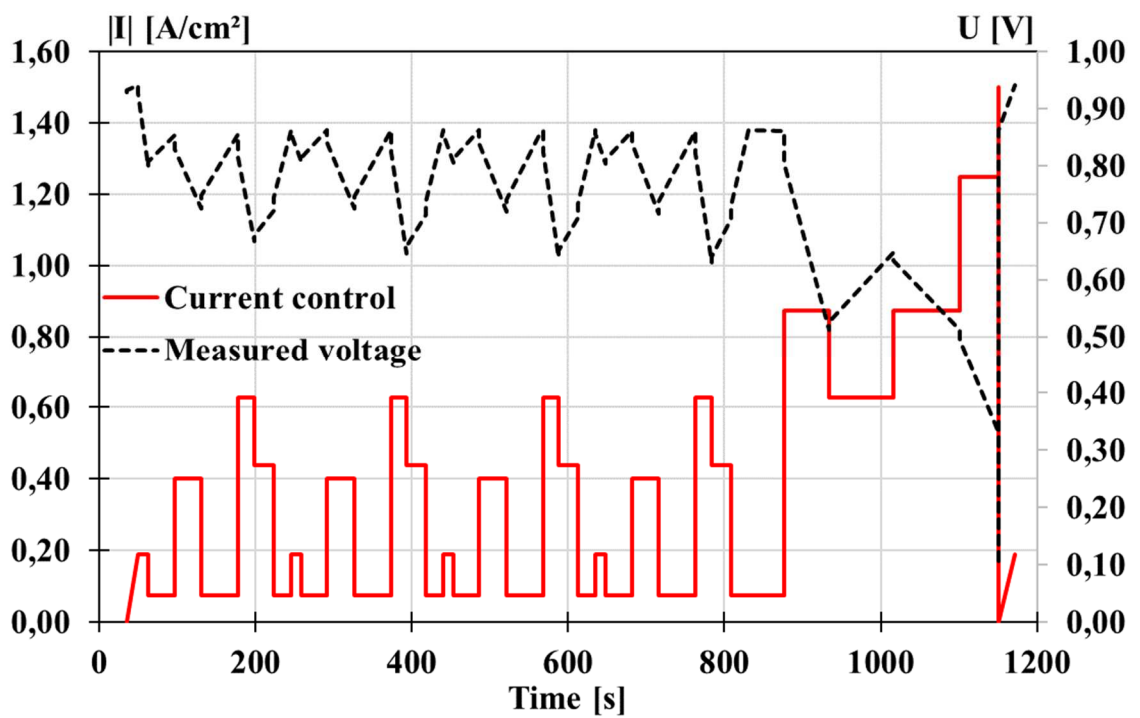
Cell temperature is controlled by a water circulation through the cell monopolar plates. Gas supply tubing are connected on top of the cell, and heated to avoid undesired water condensation upstream of the cell. This is mandatory to control the dew point of the inlet gas, and thus the relative humidity (RH) in the cell. Gases are evacuated at the bottom of the cell in order to flush easily liquid water without affecting fuel cell operation. The inlet dew point is controlled and varied by bubbling the gas in water at given temperature. Before recording the performance, the fuel cell needs to be conditioned, especially to hydrate the polymer of the membrane and the electrodes in order to reach an optimized membrane electrode assembly (MEA) functioning. Conditioning is done under constant H<sub>2</sub>/Air flows (38/95 Nl/h) at 0.650V, 80°C, 50% relative humidity for three hours. Polarization (I-V, current-voltage) curves are then recorded at 80°C, 98% and 100% relative humidity (wet atmosphere). The voltage or current is controlled with Bio-Logic VSP potentiostat and 20A HCV booster, using the EC-Lab software. These test conditions are chosen to be close to real operating conditions, as the on field operating temperature of fuel cells is around 80°C. Fuel cell testing are operated at relative humidity (RH) of 98% and 100%. Firstly, a relative humidity of 100% is chosen because, according to the literature [7], [44], microporous layer seems to play a major role in presence of liquid water. In addition, liquid water is present in stack at 100% RH. A relative humidity of 98% has been chosen to evaluate fuel cell performance when hydrated but with a lower risk of water stacking in the cell. Moreover, measurements are conducted at low pressure, namely 1 to 1.7 bar, targeted for automotive applications. Testing the gas diffusion layers in these restrictive conditions is useful to be representative of the working conditions of real fuel cell applications, and then allows to validate the technological interest of the new material.

A Gore Primea three-layer membrane-electrode assembly containing platinum catalyst (0.2mg<sub>Pt</sub> at the anode and 0.4mg<sub>Pt</sub> at the cathode) for the electrochemical conversion is used for the fuel cell tests. GDLs are positioned on both sides of the MEA to form a complete assembly, as shown in *Figure 1*. They are either reference GDL, or GDM with carbon nanotubes forests. A 25µm thick ethylene tetrafluoroethylene (ETFE) foil is used as sub gasket to reinforce the MEA. A 100-150µm PTFE foil is used as a gasket and mechanical

shim, depending on the thickness of the GDL, to reach a final compression ratio of 25% of the GDL. This corresponds roughly to a homogeneous stress ranging between 1 and 1.5 MPa on the whole surface of the MEA. The microporous layer is always placed facing the catalyst layer. As presented in the introduction the microporous layer makes the transition between the gas diffusion media with large pores and the catalyst layer with sub-micrometer pores, giving to the overall assembly a porosity gradient. For that matter, the side of the gas diffusion media covered by carbon nanotubes is placed facing the cathode catalyst layer. We chose to use a commercial gas diffusion with a microporous layer on the anode side. Regarding the literature, the cathode configuration mainly influences water management in the PEMFC, which is why CNTs are here studied on the cathode side. SGL 29BC, which has a similar structure as 28BC is the best state-of-the-art material, and will be used both at the anode and at the cathode as a reference test.

A durability test in a differential cell was also conducted. The membrane electrode assembly was prepared as in the electrochemical test previously described, with the same MEA and working surface area (1.8cm<sup>2</sup>). The durability test run for 100 hours, at 80°C for the cell temperature, and 80%RH with air (cathode) and hydrogen (anode) gas flows. Gas flows are 600ml/min at the anode at 2.5bar and 630 ml/min at the cathode at 2.3bar. The durability test consists in successive cycles in current of 20 minutes each between open circuit voltage (OCV) i.e voltage at 0A and 1.25A/cm<sup>2</sup>, known as Fuel Cell Dynamic Load Cycle, (FC-DLC) and described in ref [45]. *Figure 3* depicts the current set points used during one typical durability test cycle, with the cell measured voltage for each set point. As seen on *Figure 3*, the voltage response is smoother than the current control. For each set point, the voltage has to stabilize for a certain time, which explains the slopes between the measured voltage points.

Figure 3: Current set points for a durability test cycle ( \_\_\_ ) and the measured voltage for each set point ( --- ).



### 3-Results and discussion

#### 3-1 Material choice and pretreatment

Carbon nanotubes are directly grown on commercial carbon fiber based gas diffusion media free of hydrophobic treatment and microporous layer. These commercial gas diffusion media are carbon papers only made of graphitized carbon fibers, specifically chosen to comply with the carbon nanotubes growth requirements. In particular, the carbon nanotubes growth support need to withstand harsh process conditions which includes the resistance to a reductive atmosphere and temperatures up to 650°C. These requirements were detailed in section 2.1.

Thermogravimetric (TGA) analyses were conducted in order to verify that the commercial carbon papers are compatible with the carbon nanotubes growth requirements. For that matter, samples of several commercial gas diffusion media without hydrophobic treatment and without microporous layer were cured under air from room temperature to 1000°C. The weight losses of samples were recorded to quantify their degradation. Carbon paper supports like Spectracarb 2050A-0850 and Toray TGPH-060 start to be degraded at temperatures higher than 700°C and are thus suitable for our study. Carbon nanotubes growth has been successful on both Spectracarb and Toray papers. Other carbon papers such as Sigracet 28AA were tested, since they are used in this study as reference for fuel cell test when they are coated with a hydrophobic treatment and a microporous layer. Unfortunately, this carbon paper cannot withstand temperatures higher than 600°C. The selected gas diffusion media were annealed at atmospheric pressure, under air at 615°C for two hours to remove residual pollutants prior catalyst deposition and CNT growth.

### 3-2 Catalyst choice

The key to grow vertically aligned carbon nanotubes forest is to stabilize a distribution of catalytic particles with similar morphological and catalytic properties on the support. In spite of the low surface energy of the carbon fibers, the high mobility of iron catalyst on carbon leads to large diameter catalyst droplets detrimental to aligned CNT growth. Usually, metal oxides such as SiO<sub>2</sub>, MgO or Al<sub>2</sub>O<sub>3</sub> are used as carbon nanotubes supports for their stability when used with hydrocarbon gases, and their ability to stabilize catalyst nanoparticles [21]. For fuel cell application, a good electrical contact is required between the gas diffusion media and the carbon nanotubes to collect the electrons. Such oxide layers deposited on the carbon fibers would create an insulating barrier and unacceptable increase of the cell resistance. The need to create good electrical contact between carbon nanotubes and conductive substrate has been a challenge for several years as shown in [46]. To this end we are using a specific three-layer catalyst (Ti/Al/Fe, cf section 2.1) developed to grow carbon nanotubes on carbon

supports such as graphene and pyrolytic graphite [47]. Briefly, Ti promotes a good adhesion onto the carbon fiber and forms a stable titanium aluminide alloy with Al during the CNT growth process. This oxidation-resistant alloy supports the dewetting of Fe into small nanoparticles, which is key for efficient growth of aligned CNTs.

### 3-3 Carbon nanotubes growth results

*Figure 4* presents the microstructure of the CNT forests grown on the annealed Toray (*figure 4A*) and Spectracarb (*figure 4B, C, D*) commercial GDM carbon paper via the process described above. Carbon nanotubes forests were grown on the surface of the carbon fibers of the support which were exposed to catalyst deposition. The forests are oriented perpendicularly to the fiber axis. The average carbon nanotubes length is 10 $\mu$ m to 20 $\mu$ m on both carbon supports (*figure 4A & B*). This means that the orientation and shape of the carbon nanotubes layers in this study are directly related to the catalyst layer composition and to the growth process, and not to the roughness or surface chemistry of the carbon fiber. This organization is radically different from other direct growth results on carbon fibers, which resulted in fuzzy forests of carbon nanotubes all around the fibers [18], [19], [22], [23], [27], [48]–[50]. When zooming on the carbon nanotubes forests (*figure 4C*), one can notice that the carbon nanotubes arranged in bundles (*figure 4D*) are dense and parallel. This type of direct growth of aligned forests of CNTs was never demonstrated in the literature before.

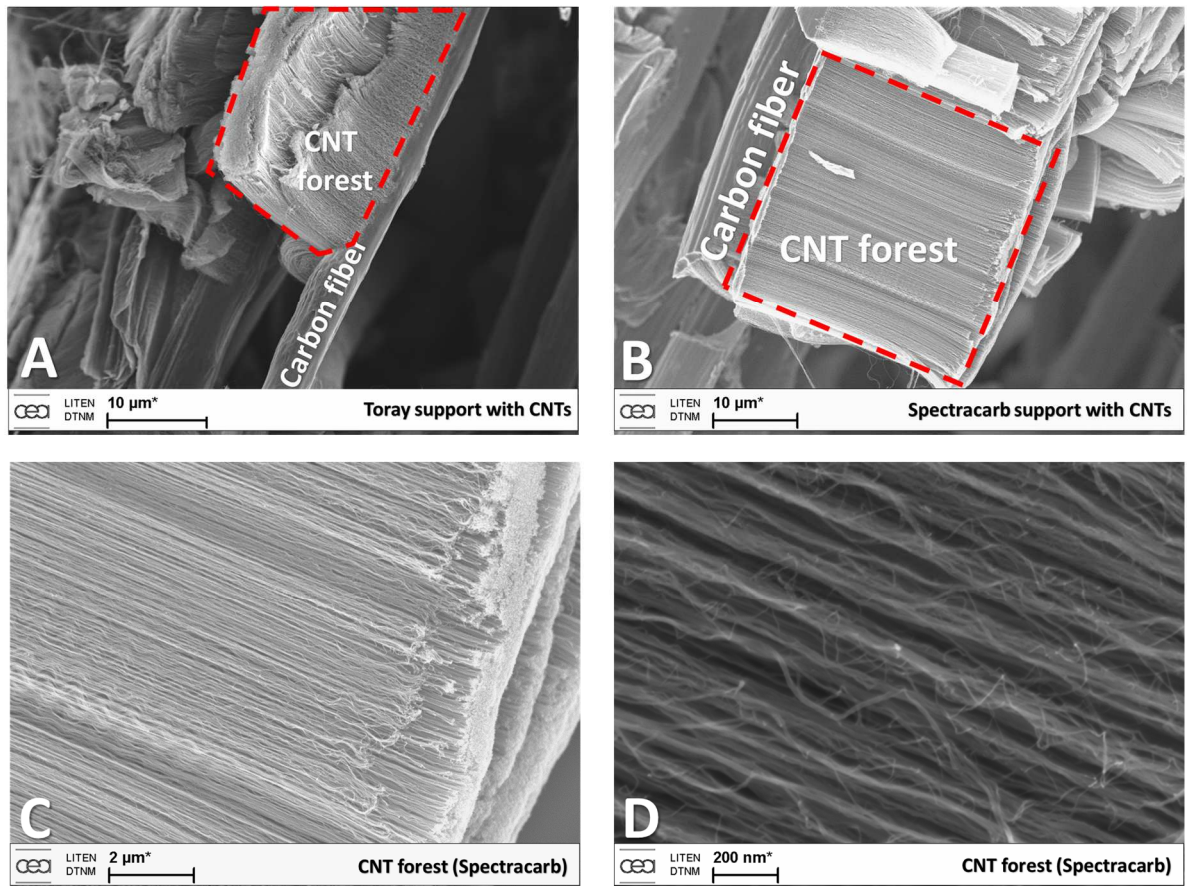


**Figure 4: SEM images of vertically aligned carbon nanotubes forests on the carbon fibers of a Toray paper (A) and Spectracarb paper (B); close side view of a carbon nanotubes forest grown on a Spectracarb support (C, D)**

TEM imaging was performed to analyze the structure and quality of the CNTs forests grown on carbon fibers. A representative TEM image is displayed in *figure 5A*. Alternation of dark lines and white lines indicates the number of walls of the nanotubes. The carbon nanotubes produced on the gas diffusion media do not have all the same diameter and number of walls. The log normal distributions of these parameters are shown on graphs *figure 5B and C*.

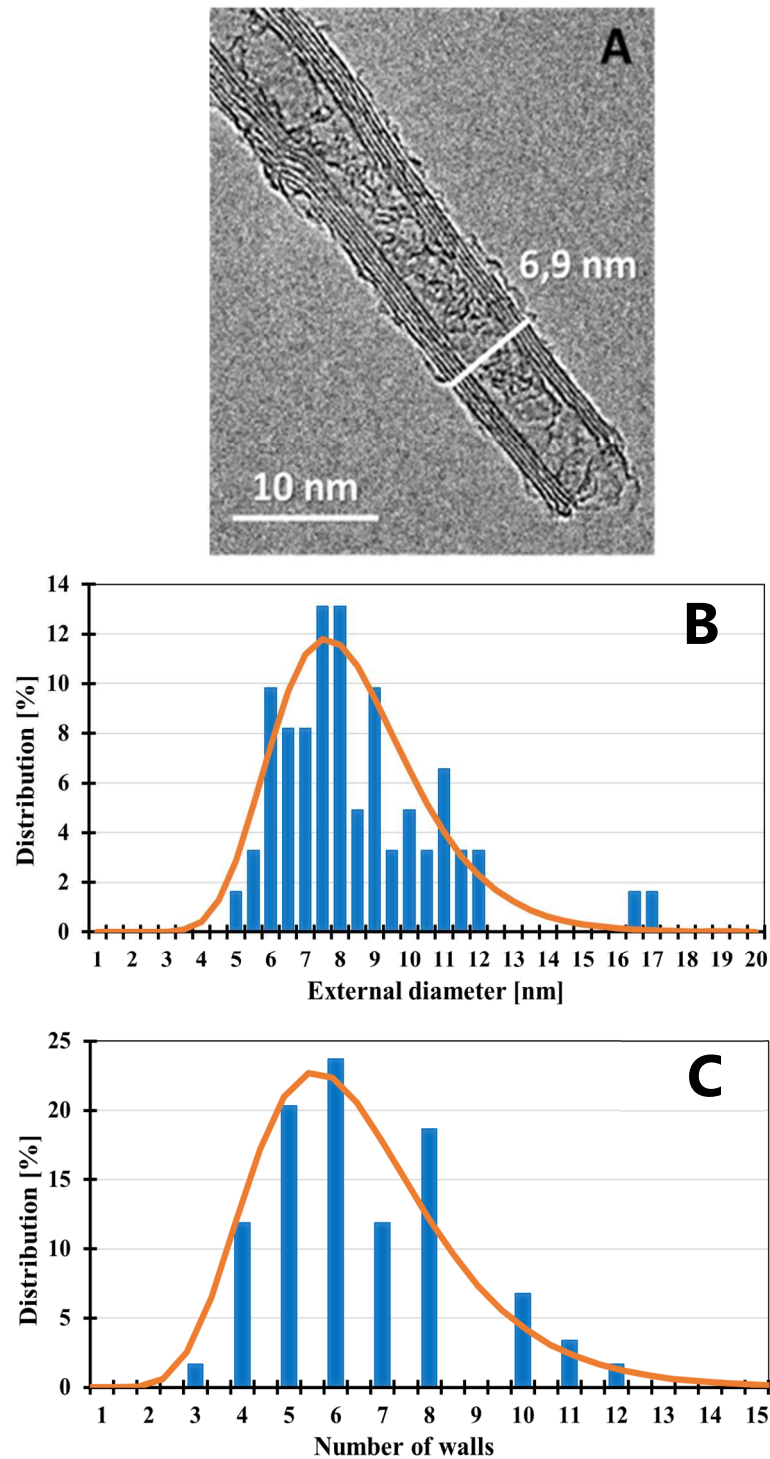


**Figure 5: A) TEM imaging of carbon nanotubes samples; B) Distribution of carbon nanotubes outer diameter and C) distribution of the walls number.**

The carbon nanotube median external diameter is 7.5 to 8 nm. This is a quite small diameter compared to other multiwall carbon nanotubes grown by CVD and HF-CVD process on carbon surface. The median number of walls is 6. The CNT diameter is directly linked to

the catalyst droplet diameter obtained during dewetting. These results show that it is possible to obtain small multiwall carbon nanotubes on carbon fibers at low temperature and low pressure and demonstrate the efficiency and stability of the three-layer catalyst.

In order to understand the microporous layer role in a PEM fuel cell and the carbon nanotubes interest as a microporous layer, it is important to compare the microstructure of a commercial microporous layer and the CNT structures developed in this study. *Figure 6* depicts the surface morphology of gas diffusion media and gas diffusion layers either with a commercial MPL or with carbon nanotubes forests.

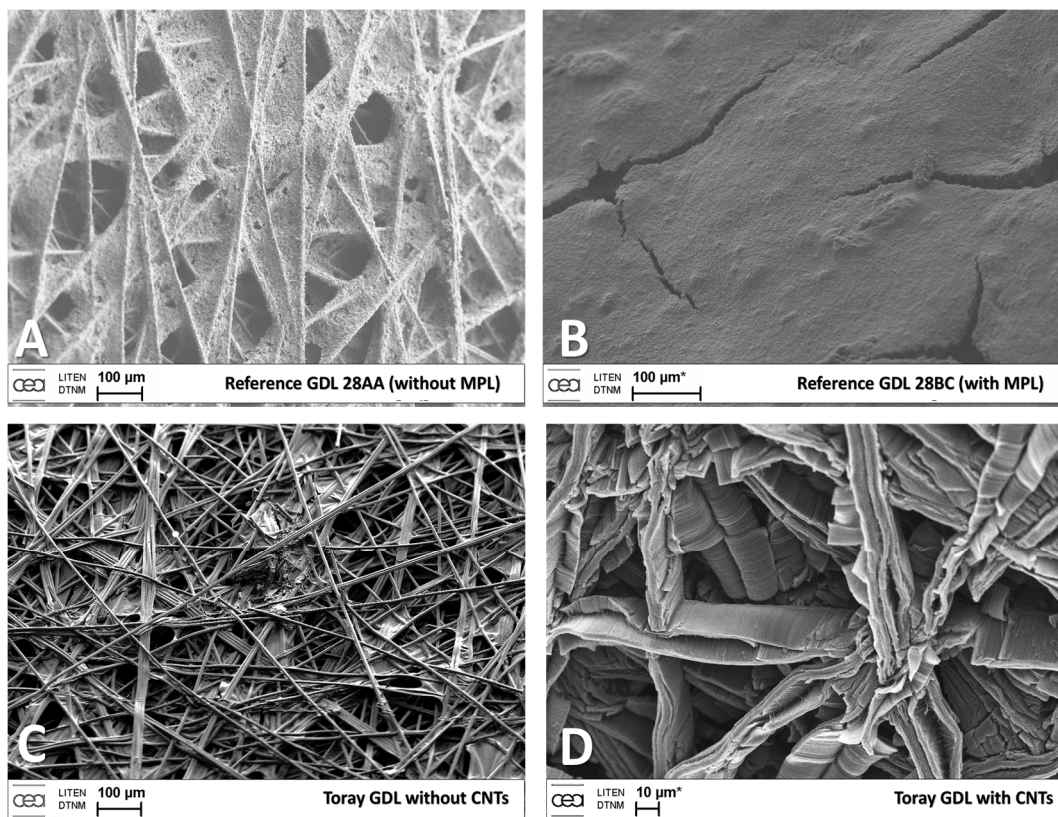


**Figure 6: SEM images of A) Sigracet 28AA reference gas diffusion media surface (without MPL); B) MPL surface of a Sigracet 28BC reference gas diffusion layer (similar to Sigracet 29BC); C) Toray gas diffusion media raw surface for CNT growth; D) Toray gas diffusion layer with CNTs forests.**

Commercial gas diffusion layers are usually composed of a gas diffusion media made mainly of carbon fibers with hydrophobic treatment based most often on fluorinated or perfluorinated polymer such as PTFE. It is coated on one side with a microporous layer

usually made of a blend of carbon black and hydrophobic polymer binder such as PTFE.. In order to compare the microstructure of commercial gas diffusion layers used as references for the electrochemical tests, *figure 6 A&B* show SEM imaging of a commercial gas diffusion layer from Sigracet 28 series. This GDL is 235  $\mu\text{m}$  thick, comprising a MPL thickness of approximately 45  $\mu\text{m}$ . Mean pore diameter of the substrate is between 0.1 to 0.3  $\mu\text{m}$  (Hg porosimetry measurements from manufacturer's data). As observed in *figure 6B* the microporous layer surface forms a quite homogeneous layer on the surface of the carbon fibers (*figure 6A*) covering the large pores of the carbon fiber media, drastically reducing the width of the visible pores. Some cracks are visible on the MPL surface. *Figure 6C* shows the organization and shape of the carbon fibers of the Toray carbon paper. Toray paper is 190  $\mu\text{m}$  thick. The carbon fibers have a diameter between 7  $\mu\text{m}$  and 10  $\mu\text{m}$ . The carbon paper is a two-dimensional network of in-plane entangled carbon fibers. This porous media possess large pores in the plane, and also large through plane pathways resulting from the connection of the in plane pores. The mean pore size of this carbon paper measured by Hg porosimetry is reported to be 0.26  $\mu\text{m}$  in [51]. These kinds of pathways are necessary for the reactant gases to reach the catalyst layer and the liquid water to be evacuated. As shown by SEM imaging in *figure 6D*, gas diffusion layers with carbon nanotubes present a heterogeneous surface, in stark contrast with *figure 5B*. As detailed above, the carbon nanotubes were only grown on the top of the carbon fibers network. The open porosity of the gas diffusion media is still accessible even after carbon nanotube growth, and it can be observed that the growth also occurred on the subsurface fibers exposed by the open pores. This distribution gives a drastically different surface than a commercial MPL (*figure 6B vs 6D*). This novel gas diffusion layer provides two kinds of through plane porosities at the same time: large pores related to the gas diffusion media structure, and small pores related to the carbon nanotubes forests structure.

Another major difference between commercial GDL and the GDM with CNTs fabricated in this study is their difference in water surface wetting behavior. Indeed, gas diffusion layers with carbon nanotubes appear to be hydrophilic, with water contact angles below 90° (see supplementary S2). This is an important difference with reference material, as commercial GDL (with or without MPL) are hydrophobic with a water contact angle around 130°. This hydrophilicity is explained by both the absence of hydrophobic agent, and by the carbon nanotube growth process that generates surface modification of the fibers due to temperature and gases.

### 3-4 Carbon nanotubes-based microporous layer integrated in a single cell

The polarization curves show the raw measured voltage as a function of current density. The current density corresponds to the raw current measurement normalized by the cell surface area of 1.8 cm<sup>2</sup>. We present two comparison. Each polarization curve is representative of the presented results, and the reproducibility of the electrochemical performances has been checked. For that matter, one result by fuel cell configuration is displayed, so that the figures are more readable. Firstly, *figure 7* compares the polarization curves of the same fuel cell configuration with and without carbon nanotubes on the gas diffusion media at the cathode. Second, *figure 8* compares a fuel cell configuration with carbon nanotubes as a MPL at the cathode side, to the reference GDL 29BC. The same curves are given in specific current (current normalized by the catalyst area) in supplementary S3, with also power density curves. The polarization curves in specific current density show that the gap between the performances of two different fuel cell configuration are not due to the ohmic drop nor from the difference in the electrochemically active surface area. This allows to evaluate the interest of carbon nanotubes as a MPL and also to compare them to a commercial MPL.

The differences between the resulting curves are linked to the ohmic drop, electrochemical phenomena such as the limiting oxygen reduction reaction (ORR), gas reactant transport and water management. At low current density, the voltage drop is mostly due to the slow kinetics of the oxygen reduction reaction [52]. At high current densities (>1 A/cm<sup>2</sup>), major losses come from gas transport limitations, that can be dramatically increased by water flooding. Actually, these losses can also be considered as ORR losses, as they come from a decrease in concentration of O<sub>2</sub> close to the catalyst area. This decrease is linked to different phenomena. In the case of high current densities, the flux of O<sub>2</sub> increase in the GDL. The quantity of water produced in this area is then also increased, which might block the pores of the GDL and prevent reactant crossing. The reactant transport limitation due to the presence of liquid water in the GDL, or even in the channels has an effective impact on the catalyst use, as the catalyst sites are not easily accessible anymore. In between these two regimes, losses are linked to the ohmic drop and the oxygen reduction reaction efficiency.

*Figure 7* depicts an overall performance improvement when using CNTs at 100% RH. Regarding those results, CNT forests play a similar role as a MPL in presence of liquid water. The voltage decay starting from 0.8 A/cm<sup>2</sup> for the configuration without CNTs might be due to the flooding of the GDL or the channels. As explained in the introduction, the current main issue for PEMFC is water management especially at high current densities [1]–[3], [53] at the

cathode side. Water flooding tends to inhibit gas transport through the porous medium of the fuel cell [7]. Then, as the way to the catalytic sites is either blocked or disadvantaged, this inhibits catalyst utilization which means a voltage drop for a given current. Here, carbon nanotube forests are able to fulfill a MPL role by limiting the water flooding consequences on performances.

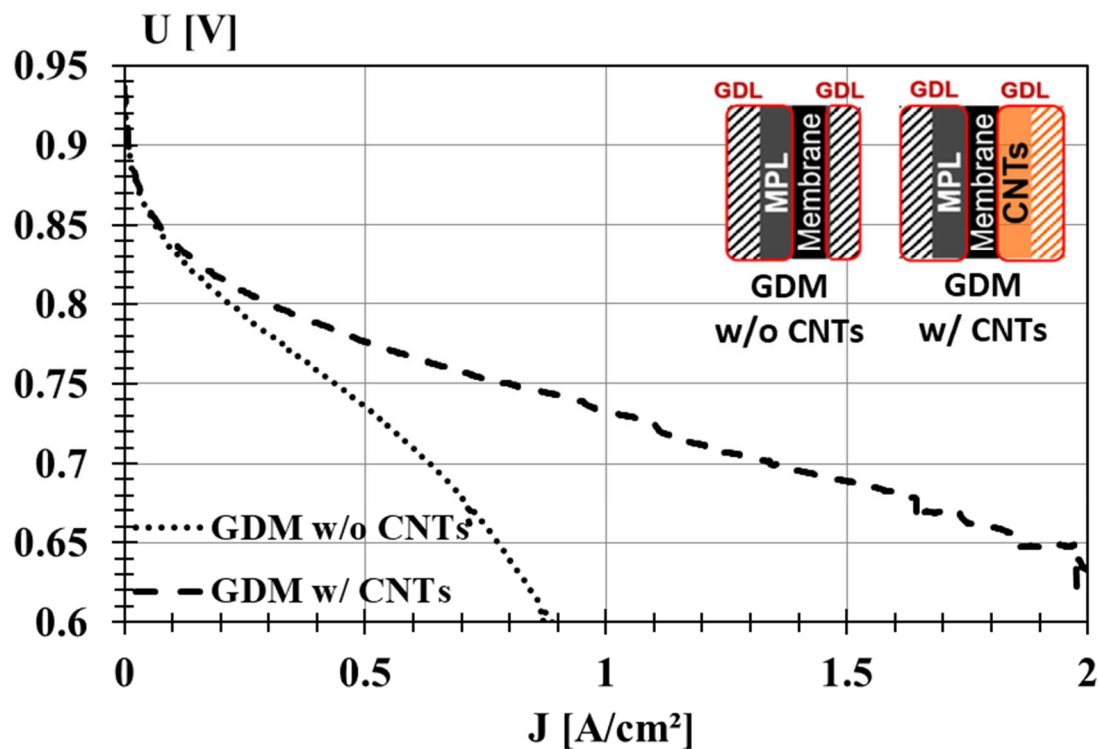


**Figure 7: Polarization curves obtained at 80°C, 100% relative humidity, under hydrogen (anode) and air (cathode) flows, showing the comparison between a Toray cathode GDM with (---) and without (...) CNT forests.**

On figure 8, the presence of carbon nanotube forest at the cathode side improves the overall fuel cell performances up to 1.7 A/cm<sup>2</sup> compared to the best state-of-the-art GDL as of today. For fuel cell applications, it is relevant to compare the electrochemical results at a given voltage, meaning at a given electrical efficiency. For the voltage point of 0.75V (50% efficiency for a fuel cell), the presence of carbon nanotubes as a MPL provides an improvement of 30%. Although the reasons for this improvement still need to be fully understood, these results show that performances similar or better than the best references can be obtained with a MPL structure drastically different than usual MPL. Even if better performances than the reference are achieved, a voltage drop occurs for the cell configuration

with CNTs at 1.74 A/cm<sup>2</sup>. The origin of this voltage drop can also be ascribed to the presence of liquid water in the pore of the GDL because of its hydrophilicity, thus blocking the access of reactants to the catalyst layer. As observed in previous part, the GDM with CNTs are hydrophilic, which might also explain this difference in water management with the reference, which is hydrophobic.

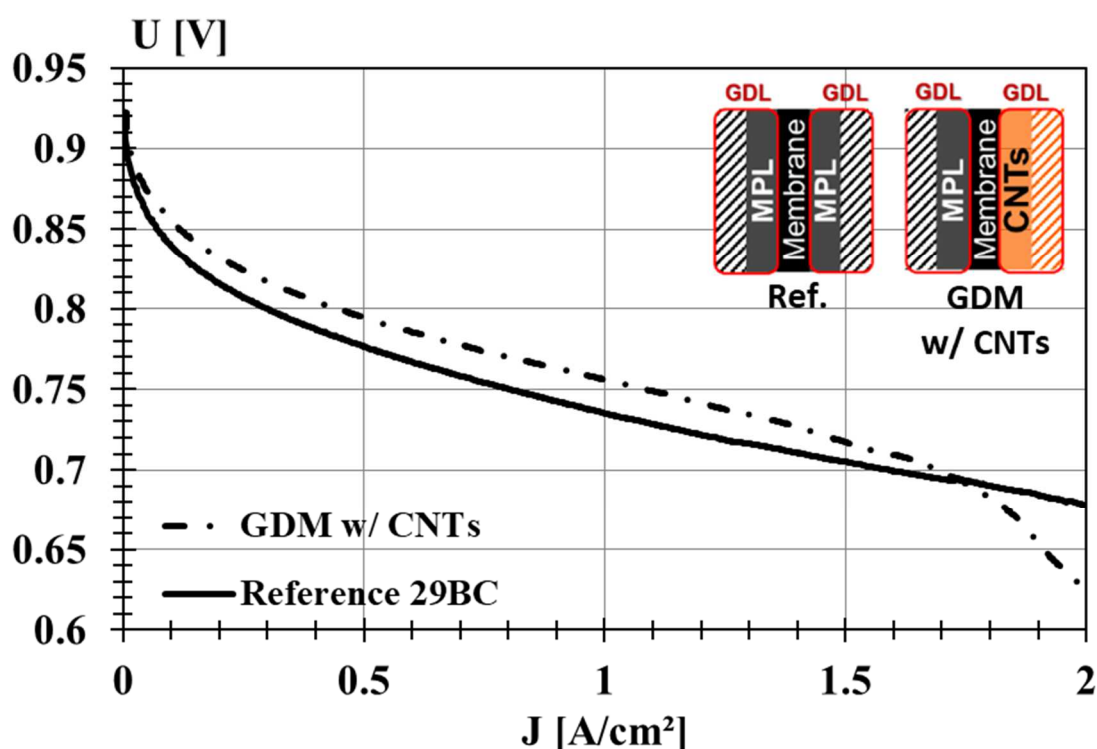


**Figure 8: Polarization curves of the single cell tests conducted at 80°C, 98% relative humidity, under hydrogen (anode) and air (cathode) flows, showing the comparison between a state of the art gas diffusion layer 29BC and a configuration with a cathode side with carbon nanotubes forests as a MPL on Toray paper.**

Carbon nanotube forests have proven their efficiency as a MPL and our results compete with current state of the art performances (see supplementary S4). It is beyond the scope of this paper and difficult for now to conclude on the main factor explaining this performance improvement and further studies are ongoing. The nanostructure of this novel MPL could play a specific role in gas or water pathways repartition through the overall gas diffusion layer, due to the orientation and the specific physical properties of carbon nanotubes forests. As described before in section 3-3, our GDL has two levels of porosity: the large pores configuration of the GDM and the porosity of the carbon nanotubes forests. Also,

carbon nanotubes could provide a different thermal management as a MPL, as thermal management in the porous media also plays a role in bettering fuel cell performances[1]–[3], [53]. The interactions between these carbon nanotubes forests and the catalytic layer are unknown, but could also interfere with the fuel cell performance. For all those aspects, directly grown carbon nanotubes forests have proven their interest as a novel structure for the improvement of fuel cell performances and a better understanding of the occurring mechanisms inside the porous media.

### 3-5 Durability test

In order to confirm the relevance of this material for long-term use in real conditions, a preliminary durability test of 100 hours was conducted. As a footprint of the degradation of the MEA, the evolution of the cell voltage at OCV ( $J=0A/cm^2$ ) and at a higher current density of  $J=0.63A/cm^2$  were extracted from the overall durability test data and are shown in Figure 9. The cell configuration is the same as in Figure 8 “GDM w/ CNTs” configuration, i.e. a reference GDL at the anode and a Toray paper with CNTs at the cathode.

The Open Circuit Voltage ( $J=0A/cm^2$ ) starts at 0.94V for  $t=0h$  and ends at 0.93V for  $t=100h$ . One can observe a stabilization around 0.93V during the last testing hours that indicates that the degradation rate is much slower. The voltage curve for  $J = 0.63A/cm^2$  has endured a larger decrease of 11% during the overall aging test. The voltage drop at  $t=79h$  (*Figure 9 inserted graph*) from 0.75V to 0.72V is related to the refilling of the gas humidifier with water, that implies to stop and restart the experiment, with switch off and on of reactant gas flow. This voltage drop is then ascribed to the detrimental effect of this procedure independently of the composition of the MEA. At higher current densities, the flows crossing the cell are more important, which explains why the degradation is more visible at  $0.63A/cm^2$  than at  $0A/cm^2$ . This is even truer because of the lack of hydrophobic treatment of our GDL, which implies a higher disposition of our cell to flooding, thus degrading the overall cell performance. It has to be noted that this is the first time that a aging test is run using a differential cell. This first aging result is encouraging as the fuel cell test conditions are quite drastic and representative of automotive applications [45]. Regarding these preliminary aging results, carbon nanotubes as a MPL could be suitable for PEMFC use. A deeper analysis however has to be driven with a longer test (at least several thousand hours) and with a hydrophobic treatment, to confirm this assumption. These analyses are beyond the scope of this paper.

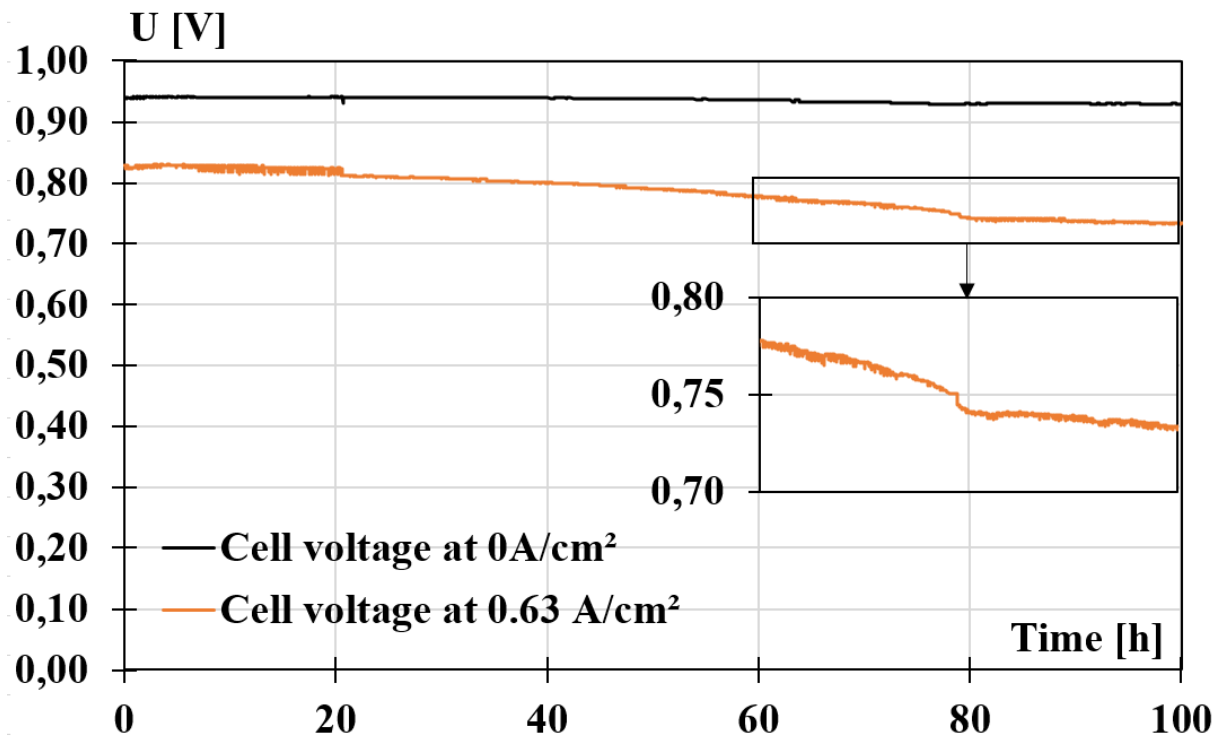


**Figure 9: Evolution of OCV (cell voltage at 0A/cm<sup>2</sup>) and cell voltage at 0.63 A/cm<sup>2</sup> during a preliminary 100 hours durability test at 80°C, 80%HR under H<sub>2</sub>/Air gas flows following FC-DLC cycle. The tested MEA is a reference GDL at the anode and a Toray with CNTs at the cathode, as in Figure 8 (named “GDM w/ CNTs”).**

#### 4-Conclusions

Vertically aligned carbon nanotubes forests were successfully synthesized on carbon papers by chemical vapor deposition assisted with hot carbon filaments. The use of carbon papers as a support, and the quality of the aligned CNT structure obtained by direct growth, strictly differs from what is observed in literature until now concerning carbon nanotubes growth on carbon fibers.

The dense carbon nanotubes forests are clearly vertically aligned and are distributed all along the carbon fibers, perpendicularly to them. The forests are composed of small multiwall carbon nanotubes, from 10  $\mu\text{m}$  to 20  $\mu\text{m}$  in length and 7.5 to 8 nm in diameter, with about 6 walls.

Regarding the electrochemical results, the aligned carbon nanotubes demonstrated their efficiency as a MPL. Performances are also at least similar to the best state of the art gas diffusion layer, and improvement up to 30% in current density was obtained at 0.75V, without any hydrophobic treatment. The first durability test of 100 hours indicates that the use of carbon nanotubes seems suitable as a microporous layer for PEMFC, as no dramatic decrease in Open Circuit Voltage (at 0A/cm<sup>2</sup>) and voltage at 0.63A/cm<sup>2</sup> has been induced by harsh load cycling representative of automotive application.

Further study needs to be conducted to give elements for a better understanding of the fundamental reasons for these performances' improvement. In particular, carbon nanotubes length and diameter can be modified to provide other MPL forests structure. Changing the length of the carbon nanotubes forests could provide further information on the nanostructure impact on the fuel cell performances. Operando neutron imaging could also be conducted to directly probe water management in a single cell using CNTs as MPL.

#### References:

- [1] C. Hartnig, I. Manke, R. Kuhn, S. Kleinau, J. Goebbels, et J. Banhart, « High-resolution in-plane investigation of the water evolution and transport in PEM fuel cells », *J. Power Sources*, vol. 188, n° 2, p. 468-474, mars 2009, doi: 10.1016/j.jpowsour.2008.12.023.
- [2] G. Gebel, O. Diat, S. Escribano, et R. Mosdale, « Water profile determination in a running PEMFC by small-angle neutron scattering », *J. Power Sources*, vol. 179, n° 1, p. 132-139, avr. 2008, doi: 10.1016/j.jpowsour.2007.12.124.
- [3] C. Quick, D. Ritzinger, W. Lehnert, et C. Hartnig, « Characterization of water transport in gas diffusion media », *J. Power Sources*, vol. 190, n° 1, p. 110-120, mai 2009, doi: 10.1016/j.jpowsour.2008.07.093.
- [4] I. Zenyuk, « Understanding Liquid-Water Management in PEFCs Using X-Ray Computed Tomography and Modeling », présenté à 228th ECS Meeting (October 11-15, 2015), oct. 2015, Consulté le: oct. 15, 2019. [En ligne]. Disponible sur: <https://ecs.confex.com/ecs/228/webprogram/Paper57529.html>.
- [5] S. Chevalier *et al.*, « Synchrotron X-ray Radiography as a Highly Precise and Accurate Method for Measuring the Spatial Distribution of Liquid Water in Operating Polymer Electrolyte Membrane Fuel Cells », *J. Electrochem. Soc.*, vol. 164, n° 2, p. F107-F114, janv. 2017, doi: 10.1149/2.0041702jes.

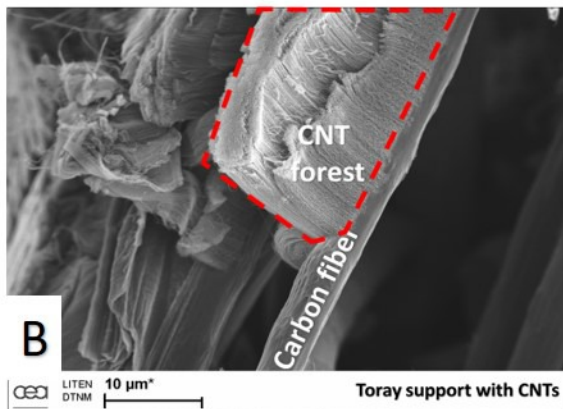
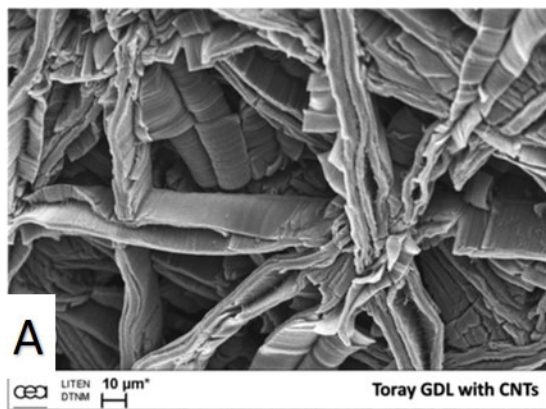
- [6] J. Eller, J. Roth, F. Marone, M. Stampanoni, et F. N. Büchi, « Operando Properties of Gas Diffusion Layers: Saturation and Liquid Permeability », *J. Electrochem. Soc.*, vol. 164, n° 2, p. F115-F126, janv. 2017, doi: 10.1149/2.0881702jes.
- [7] J. T. Gostick, M. A. Ioannidis, M. D. Pritzker, et M. W. Fowler, « Impact of Liquid Water on Reactant Mass Transfer in PEM Fuel Cell Electrodes », *J. Electrochem. Soc.*, vol. 157, n° 4, p. B563-B571, janv. 2010, doi: 10.1149/1.3291977.
- [8] P. Oberholzer et P. Boillat, « Local Characterization of PEFCs by Differential Cells: Systematic Variations of Current and Asymmetric Relative Humidity », *J. Electrochem. Soc.*, vol. 161, n° 1, p. F139-F152, janv. 2014, doi: 10.1149/2.080401jes.
- [9] N. Jung, D. Y. Chung, J. Ryu, S. J. Yoo, et Y.-E. Sung, « Pt-based nanoarchitecture and catalyst design for fuel cell applications », *Nano Today*, vol. 9, n° 4, p. 433-456, août 2014, doi: 10.1016/j.nantod.2014.06.006.
- [10] R. Lin, X. Diao, T. Ma, S. Tang, L. Chen, et D. Liu, « Optimized microporous layer for improving polymer exchange membrane fuel cell performance using orthogonal test design », *Appl. Energy*, vol. 254, p. 113714, nov. 2019, doi: 10.1016/j.apenergy.2019.113714.
- [11] Y. Nagai *et al.*, « Improving water management in fuel cells through microporous layer modifications: Fast operando tomographic imaging of liquid water », *J. Power Sources*, vol. 435, p. 226809, sept. 2019, doi: 10.1016/j.jpowsour.2019.226809.
- [12] O. M. Orogbemi, D. B. Ingham, M. S. Ismail, K. J. Hughes, L. Ma, et M. Pourkashanian, « The effects of the composition of microporous layers on the permeability of gas diffusion layers used in polymer electrolyte fuel cells », *Int. J. Hydrog. Energy*, vol. 41, n° 46, p. 21345-21351, déc. 2016, doi: 10.1016/j.ijhydene.2016.09.160.
- [13] R. Schweiss, M. Steeb, P. M. Wilde, et T. Schubert, « Enhancement of proton exchange membrane fuel cell performance by doping microporous layers of gas diffusion layers with multiwall carbon nanotubes », *J. Power Sources*, vol. 220, p. 79-83, déc. 2012, doi: 10.1016/j.jpowsour.2012.07.078.
- [14] S.-Y. Lin et M.-H. Chang, « Effect of microporous layer composed of carbon nanotube and acetylene black on polymer electrolyte membrane fuel cell performance », *Int. J. Hydrog. Energy*, vol. 40, n° 24, p. 7879-7885, juin 2015, doi: 10.1016/j.ijhydene.2014.10.146.
- [15] G.-B. Jung, W.-J. Tzeng, T.-C. Jao, Y.-H. Liu, et C.-C. Yeh, « Investigation of porous carbon and carbon nanotube layer for proton exchange membrane fuel cells », *Appl. Energy*, vol. 101, p. 457-464, janv. 2013, doi: 10.1016/j.apenergy.2012.08.045.
- [16] T. Kitahara, H. Nakajima, et K. Okamura, « Gas diffusion layers coated with a microporous layer containing hydrophilic carbon nanotubes for performance enhancement of polymer electrolyte fuel cells under both low and high humidity conditions », *J. Power Sources*, vol. 283, p. 115-124, juin 2015, doi: 10.1016/j.jpowsour.2015.02.115.
- [17] J. Lee *et al.*, « Multiwall Carbon Nanotube-Based Microporous Layers for Polymer Electrolyte Membrane Fuel Cells », *J. Electrochem. Soc.*, vol. 164, n° 12, p. F1149-F1157, janv. 2017, doi: 10.1149/2.0861712jes.
- [18] C. Du, B. Wang, et X. Cheng, « Hierarchy carbon paper for the gas diffusion layer of proton exchange membrane fuel cells », *J. Power Sources*, vol. 187, n° 2, p. 505-508, févr. 2009, doi: 10.1016/j.jpowsour.2008.11.046.

- [19] A. M. Kannan, P. Kanagala, et V. Veedu, « Development of carbon nanotubes based gas diffusion layers by in situ chemical vapor deposition process for proton exchange membrane fuel cells », *J. Power Sources*, vol. 192, n° 2, p. 297-303, juill. 2009, doi: 10.1016/j.jpowsour.2009.03.022.
- [20] R. J. Cartwright *et al.*, « The role of the sp<sup>2</sup>:sp<sup>3</sup> substrate content in carbon supported nanotube growth », *Carbon*, vol. 75, p. 327-334, août 2014, doi: 10.1016/j.carbon.2014.04.011.
- [21] Z. Gao et M. M. F. Yuen, « Study of CNT growth termination mechanism: Effect of catalyst diffusion », in *2012 13th International Thermal, Mechanical and Multi-Physics Simulation and Experiments in Microelectronics and Microsystems*, avr. 2012, p. 1/5-5/5, doi: 10.1109/ESimE.2012.6191723.
- [22] S. Zhu, C.-H. Su, S. L. Lehoczky, I. Muntele, et D. Ila, « Carbon nanotube growth on carbon fibers », *Diam. Relat. Mater.*, vol. 12, n° 10, p. 1825-1828, oct. 2003, doi: 10.1016/S0925-9635(03)00205-X.
- [23] Z.-G. Zhao, L.-J. Ci, H.-M. Cheng, et J.-B. Bai, « The growth of multi-walled carbon nanotubes with different morphologies on carbon fibers », *Carbon*, vol. 43, n° 3, p. 663-665, janv. 2005, doi: 10.1016/j.carbon.2004.10.013.
- [24] J. Zhao *et al.*, « Growth of carbon nanotubes on the surface of carbon fibers », *Carbon*, vol. 46, n° 2, p. 380-383, févr. 2008, doi: 10.1016/j.carbon.2007.11.021.
- [25] T. R. Pozegic *et al.*, « Low temperature growth of carbon nanotubes on carbon fibre to create a highly networked fuzzy fibre reinforced composite with superior electrical conductivity », *Carbon*, vol. 74, p. 319-328, août 2014, doi: 10.1016/j.carbon.2014.03.038.
- [26] W. Fan *et al.*, « Controllable growth of uniform carbon nanotubes/carbon nanofibers on the surface of carbon fibers », *RSC Adv.*, vol. 5, n° 92, p. 75735-75745, sept. 2015, doi: 10.1039/C5RA15556H.
- [27] J. Sun, H. Li, L. Han, et Q. Song, « Growth of radially aligned porous carbon nanotube arrays on pyrolytic carbon coated carbon fibers », *Vacuum*, vol. 164, p. 170-174, juin 2019, doi: 10.1016/j.vacuum.2019.03.005.
- [28] K.-H. Kim, A. Gohier, J. E. Bourée, M. Châtelet, et C.-S. Cojocar, « The role of catalytic nanoparticle pretreatment on the growth of vertically aligned carbon nanotubes by hot-filament chemical vapor deposition », *Thin Solid Films*, vol. 575, p. 84-91, janv. 2015, doi: 10.1016/j.tsf.2014.10.013.
- [29] N. T. Hong, K. H. Koh, N. T. T. Tam, P. N. Minh, P. H. Khoi, et S. Lee, « Combined model for growing mechanism of carbon nanotubes using HFCVD: effect of temperature and molecule gas diffusion », *Thin Solid Films*, vol. 517, n° 12, p. 3562-3565, avr. 2009, doi: 10.1016/j.tsf.2009.01.066.
- [30] Th. Dikonimos Makris *et al.*, « Carbon nanotubes growth by HFCVD: effect of the process parameters and catalyst preparation », *Diam. Relat. Mater.*, vol. 13, n° 2, p. 305-310, févr. 2004, doi: 10.1016/j.diamond.2003.10.013.
- [31] Z. P. Huang, J. W. Xu, Z. F. Ren, J. H. Wang, M. P. Siegal, et P. N. Provencio, « Growth of highly oriented carbon nanotubes by plasma-enhanced hot filament chemical vapor deposition », *Appl. Phys. Lett.*, vol. 73, n° 26, p. 3845, déc. 1998, doi: 10.1063/1.122912.

- [32] K.-H. Kim, E. Lefeuvre, M. Châtelet, D. Pribat, et C. S. Cojocaru, « Laterally organized carbon nanotube arrays based on hot-filament chemical vapor deposition », *Thin Solid Films*, vol. 519, n° 14, p. 4598-4602, mai 2011, doi: 10.1016/j.tsf.2011.01.334.
- [33] L. Marty *et al.*, « Self-assembled single wall carbon nanotube field effect transistors and AFM tips prepared by hot filament assisted CVD », *Thin Solid Films*, vol. 501, n° 1, p. 299-302, avr. 2006, doi: 10.1016/j.tsf.2005.07.218.
- [34] T. Okazaki et H. Shinohara, « Synthesis and characterization of single-wall carbon nanotubes by hot-filament assisted chemical vapor deposition », *Chem. Phys. Lett.*, vol. 376, n° 5, p. 606-611, juill. 2003, doi: 10.1016/S0009-2614(03)01042-X.
- [35] S. Chaisitsak, A. Yamada, et M. Konagai, « Hot filament enhanced CVD synthesis of carbon nanotubes by using a carbon filament », *Diam. Relat. Mater.*, vol. 13, n° 3, p. 438-444, mars 2004, doi: 10.1016/S0925-9635(03)00572-7.
- [36] B. Xin *et al.*, « Carbon fiber-promoted activation of catalyst for efficient growth of single-walled carbon nanotubes », *Carbon*, vol. 156, p. 410-415, janv. 2020, doi: 10.1016/j.carbon.2019.09.089.
- [37] S. Liatard, K. Benhamouda, A. Fournier, R. Ramos, C. Barchasz, et J. Dijon, « Vertically-aligned carbon nanotubes on aluminum as a light-weight positive electrode for lithium-polysulfide batteries », *Chem. Commun.*, vol. 51, n° 36, p. 7749-7752, 2015, doi: 10.1039/C4CC08848D.
- [38] Y. Dini, J. Faure-Vincent, et J. Dijon, « How to overcome the electrical conductivity limitation of carbon nanotube yarns drawn from carbon nanotube arrays », *Carbon*, vol. 144, p. 301-311, avr. 2019, doi: 10.1016/j.carbon.2018.12.041.
- [39] G. Zhang, L. Guo, L. Ma, et H. Liu, « Simultaneous measurement of current and temperature distributions in a proton exchange membrane fuel cell », *J. Power Sources*, vol. 195, n° 11, p. 3597-3604, juin 2010, doi: 10.1016/j.jpowsour.2009.12.016.
- [40] M. Noponen, T. Mennola, M. Mikkola, T. Hottinen, et P. Lund, « Measurement of current distribution in a free-breathing PEMFC », *J. Power Sources*, vol. 106, n° 1, p. 304-312, avr. 2002, doi: 10.1016/S0378-7753(01)01063-1.
- [41] Y. Yu *et al.*, « Current mapping of a proton exchange membrane fuel cell with a segmented current collector during the gas starvation and shutdown processes », *Int. J. Hydrog. Energy*, vol. 37, n° 20, p. 15288-15300, oct. 2012, doi: 10.1016/j.ijhydene.2012.07.023.
- [42] Y.-G. Yoon, W.-Y. Lee, T.-H. Yang, G.-G. Park, et C.-S. Kim, « Current distribution in a single cell of PEMFC », *J. Power Sources*, vol. 118, n° 1, p. 193-199, mai 2003, doi: 10.1016/S0378-7753(03)00093-4.
- [43] L. Guétaz, S. Escribano, et O. Sicardy, « Study by electron microscopy of proton exchange membrane fuel cell membrane-electrode assembly degradation mechanisms: Influence of local conditions », *J. Power Sources*, vol. 212, p. 169-178, août 2012, doi: 10.1016/j.jpowsour.2012.03.096.
- [44] F. S. Nanadegani, E. N. Lay, et B. Sunden, « Effects of an MPL on water and thermal management in a PEMFC », *Int. J. Energy Res.*, vol. 43, n° 1, p. 274-296, 2019, doi: 10.1002/er.4262.

- [45] G. Tsotridis, A. Pilenga, G. De Marco, T. Malkow, European Commission, et Joint Research Centre, *EU harmonised test protocols for PEMFC MEA testing in single cell configuration for automotive applications*. Luxembourg: Publications Office, 2015.
- [46] N. Zhao et J. Kang, « Direct Growth of Carbon Nanotubes on Metal Supports by Chemical Vapor Deposition », *Carbon Nanotub. - Synth. Charact. Appl.*, juill. 2011, doi: 10.5772/19275.
- [47] H. Okuno, R. Ramos, et J. Dijon, « Substrate that is electrically conductive on at least one of the faces of same provided with a stack of thin layers for growing carbon nanotubes », FR 3006237 US 10,370,759.
- [48] S. Kaushal, A. K. Sahu, M. Rani, et S. R. Dhakate, « Multiwall carbon nanotubes tailored porous carbon fiber paper-based gas diffusion layer performance in polymer electrolyte membrane fuel cell », *Renew. Energy*, vol. 142, p. 604-611, nov. 2019, doi: 10.1016/j.renene.2019.04.096.
- [49] Z. Tang, C. K. Poh, Z. Tian, J. Lin, H. Y. Ng, et D. H. C. Chua, « In situ grown carbon nanotubes on carbon paper as integrated gas diffusion and catalyst layer for proton exchange membrane fuel cells », *Electrochimica Acta*, vol. 56, n° 11, p. 4327-4334, avr. 2011, doi: 10.1016/j.electacta.2011.01.035.
- [50] Z. Xie *et al.*, « Carbon nanotubes grown in situ on carbon paper as a microporous layer for proton exchange membrane fuel cells », *Int. J. Hydrog. Energy*, vol. 40, n° 29, p. 8958-8965, août 2015, doi: 10.1016/j.ijhydene.2015.04.129.
- [51] A. El-kharouf, T. J. Mason, D. J. L. Brett, et B. G. Pollet, « Ex-situ characterisation of gas diffusion layers for proton exchange membrane fuel cells », *J. Power Sources*, vol. 218, p. 393-404, nov. 2012, doi: 10.1016/j.jpowsour.2012.06.099.
- [52] C. Li *et al.*, « Emerging Pt-based electrocatalysts with highly open nanoarchitectures for boosting oxygen reduction reaction », *Nano Today*, vol. 21, p. 91-105, août 2018, doi: 10.1016/j.nantod.2018.06.005.
- [53] P. Huguet, A. Morin, G. Gebel, S. Deabate, A. K. Sutor, et Z. Peng, « In situ analysis of water management in operating fuel cells by confocal Raman spectroscopy », *Electrochem. Commun.*, vol. 13, n° 5, p. 418-422, mai 2011, doi: 10.1016/j.elecom.2011.02.008.

# GDL surface with CNTs (A) and CNTs alignment (B)



## Electrochemical performances

